

STRUCTURES FOR CONSTRUCTING DEVICES FROM FORMED Mn_4Si_7 AND CoSi FILMS

M.T. Normuradov¹, I.R. Bekpulatov², G.T. Imanova^{3*}, B.D. Igamov⁴

¹Karshi State University, Karshi, Uzbekistan

²Tashkent State Technical University, Tashkent, Uzbekistan

³Institute of Radiation Problems, Minister of Science and Education Republic of Azerbaijan, Baku, Azerbaijan

⁴Scientific and technical center with a design bureau and pilot production of the Academy of Sciences of the Republic of Uzbekistan, Tashkent, Uzbekistan

Abstract. This work provides information on the formation of the main part of thermal radiation receivers. In addition, the article defines and creates optimal modes for creating targets for magnetron sputtering from higher manganese silicide (Mn_4Si_7) and cobalt monosilicide (CoSi). As is known, the device is formed from a two-type film, where the Mn_4Si_7 film gives the *p*-type, and the CoSi film gives the *n*-type. Films were formed using these targets by magnetron sputtering and their electrophysical properties were studied. The results obtained showed that the resulting films have a structure suitable for instrumentation. The paper also presents theoretical studies on the creation of photomasks to create a device design. Using the method of magnetron sputtering, a structure was created that can be used in thermal radiation receivers. The mechanism of structure formation has been developed.

Keywords: Magnetron sputtering, higher manganese silicide, cobalt monosilicide, instrumentation, thermal radiation receiver, photomask.

***Corresponding Author:** G.T. Imanova, Institute of Radiation Problems, Minister of Science and Education Republic of Azerbaijan, Baku, AZ-1143, Azerbaijan, e-mail: gunel_imanova55@mail.ru

Received: 20 October 2022;

Accepted: 22 November 2022;

Published: 30 December 2022.

1. Introduction

In recent years, instrumentation has been developing very rapidly, with the greatest changes occurring in electronics and computer science. The problem of increasing the efficiency and stability of inexpensive solar cells based on amorphous silicon has been relevant for decades. Interest in solar cells obtained by low-temperature methods is primarily due to the possibility of using non-refractory substrates, as well as their moderate cost based on the use of *p-n* structures. It is known that the presence of ~ (10-15)% nanocrystalline silicon (*n* - Si) in Si suppresses the Stebler-Wronsky effect and thereby increases the stability of solar cells (Fei *et al.*, 2021; Vaqueiro & Powell, 2010; Shakouri, 2011; Morita *et al.*, 2006; Kishino *et al.*, 2007; Imai & Kikegawa, 2003; Hashimoto *et al.*, 2007; Hashimoto *et al.*, 2008; Fedorov *et al.*, 1991; Asanabe *et al.*, 1964).

How to cite (APA): Normuradov, M.T., Bekpulatov, I.R., Imanova, G.T., & Igamov, B.D. (2022). Structures for constructing devices from formed Mn_4Si_7 and CoSi films. *Advanced Physical Research*, 4(3), 142-154.

p - *n* - transition - a region of space at the junction of two semiconductors *p* - and *n* - type, in which there is a transition from one type of conductivity to another, such a transition is also called an electron-hole transition. This property of semiconductors is widely used in instrumentation. In this section of the article, we will reveal a method for creating chamomile-shaped device structures from films of higher manganese silicide and *n*-type cobalt silicide (Pshenay-Severin *et al.*, 2018; Yoneyama *et al.*, 2013; Dubov, 2019).

The pressure behavior of the competing intra- and interchain magnetic interactions was analyzed on the basis of obtained structural data and their role in the formation of the magnetic phase diagram is discussed. The pressure behavior of the Néel temperature of the commensurate AFM phase was evaluated within the mean field theory approach and a good agreement with the experimental value $dT_{NC}/dP = 0.65$ K/GPa was obtained. The samples were analysed using X-ray diffraction (XRD) and Energy dispersive spectroscopy (EDS) to study the microstructural and composition changes. The XRD results showed the crystalline structure for the sample before and after irradiation (with gamma irradiation dose 9.7, 48.5 and 97 kGy). Amorphization of the sample began at the gamma irradiation dose of 145.5 kGy. Increase in gamma irradiation dose had an inverse effect on the activation energy and had a directly proportional effect on the lattice volume (Rysbaev *et al.*, 2017a, 2017b; Kamilov *et al.*, 2019; Normurodov *et al.*, 2021; Umirzakov *et al.*, 2017, 2022; Donaev *et al.*, 2015a, 2015b).

The effect of preliminary radiation-oxidative treatment on the current density and current–voltage characteristic of metallic zirconium has been studied. The contribution of preliminary radiation-oxidative treatment to the change in the electrophysical characteristics during thermal and radiation–thermal tests in the contact of zirconium with water is revealed (Imanova & Bekpulatov, 2021; Agayev *et al.*, 2022).

The X-ray diffraction (XRD) spectrum of the nano-ZrO₂ compound was drawn, the crystal structure was determined at room temperature and under normal conditions. Radiation-thermal decomposition of water on nanosized ZrO₂ in the temperature range of $T = 300$ -673 K has been studied by Fourier transform infrared spectroscopy (FTIR) and Raman spectroscopy (Imanova *et al.*, 2021).

The paper reports on a method of low-temperature vacuum-thermal cleaning of the surface of Si and GaAs single crystals developed by the authors, which consists in implanting Ba⁺ ions (or alkaline elements) into Si and GaAs crystals preliminarily cleaned by ultra-high vacuum by ion etching and subsequent annealing in two stage at 800 K - 15 minutes and at 1000 K for 30 minutes. The effect of effective cleaning is achieved due to the fact that the introduced ions of Ba⁺ and alkaline elements, being active, form compounds with impurity atoms (O, C, S, N, etc.) at the first stage and are removed together with impurities after the second stage of heating (Tursunmetova *et al.*, 2022).

Arises formation of thin films of cobalt monosilicide (CoSi) deposited into the base surface of SiO₂/Si (111) using magnetron ion-plasma sputtering and subsequent thermal annealing. It was found that, in addition to the formation of CoSi silicide, there are also Co and Si atoms that do not form bonds on the surface. Therefore, in this work, we studied the surface morphology and composition of a CoSi silicon target using a scanning electron microscope. The study, silicide CoSi was chosen as the target and standard SiO₂/Si (111) was used as the substrate. Has been study, surface morphology and composition of the CoSi silicon film obtained by SEM. The paper reports on a method, morphology of the surface of a CoSi silicon film obtained using Raman microscopy. The results obtained are

based on the fact that they were obtained using a modern magnetron sputterer, a high-vacuum thermal heater, and modern devices (Bekpulatov *et al.*, 2022).

2. Materials and Methods

The magnetron sputtering method has been mainly used for surface research and analysis, surface cleaning, ion beam etching, discharge tube behavior, ion accelerator technology, vacuum plant design, first wall problem in fusion energy devices, space research, etc. Only after As the sputtering process itself was combined with magnetic fields (hence the term "magnetron") to improve "sputtering performance", the technique became used worldwide in a wider area of industrial applications such as deposition of thin films on various materials.

Before the introduction of the Ar^+ gas into the chamber, the pressure generated in the chamber is about 10^{-6} Pa, and the pressure of the vacuum created after the introduction of the gas is 10^{-4} Pa. The creation of targets for magnetron sputtering requires a high-tech process. In particular, metals and semiconductors are crushed to a state of powder, the required amount of which is accurately measured using an analytical balance and baked in a mold (Klechkovskaya *et al.*, 2021; Tahir *et al.*, 2020).

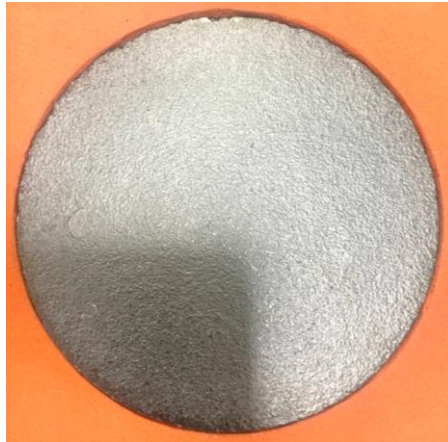


Fig. 1. Target *p* - type Mn_4Si_7



Fig. 2. Target *n* - type CoSi

The formation of the p-type Mn_4Si_7 target was carried out at a vacuum of 10^{-2} Pa by slowly heating under pressure to a maximum temperature of $1100\text{ }^\circ\text{C}$, at which it was kept for 1 hour. A constant pressure of $1.5 \cdot 10^6$ Pa was applied to the target surface. After turning off the furnace, the target was cooled to the initial state (Fig. 1). The n-type CoSi target was formed in a vacuum of 10^{-2} Pa. In this case, the manufactured target was slowly heated at a constant pressure of $1.5 \cdot 10^6$ Pa to a maximum temperature of $1050\text{ }^\circ\text{C}$. Exposure lasted 1 hour. After turning off the furnace, the sample was cooled to the initial state, and in this case, targets 76 mm in diameter and 6 mm thick were formed (Fig. 2).

Before placing the target on the magnetron, their composition and structure were examined with a Quanta 200 3D scanning electron microscope (Fig. 3 and 4). After the formation of a Mn_4Si_7 film with a thickness of $\sim 0.7\text{ }\mu\text{m}$, their resistivity was determined by the four-probe method, and the thermo-EMF, in a vacuum of 10 Pa, by the two-probe method (Mavrokefalos *et al.*, 2007).

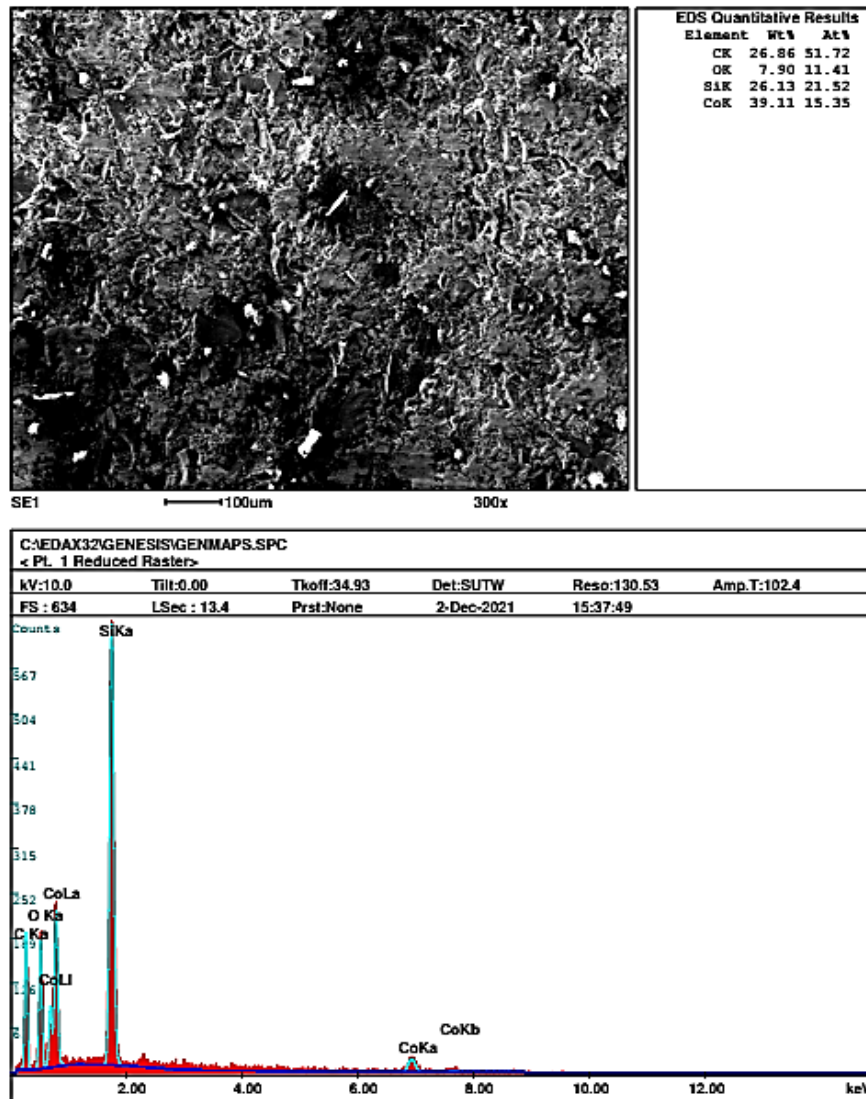


Fig. 3. Image of the CoSi target obtained with a scanning electron microscope

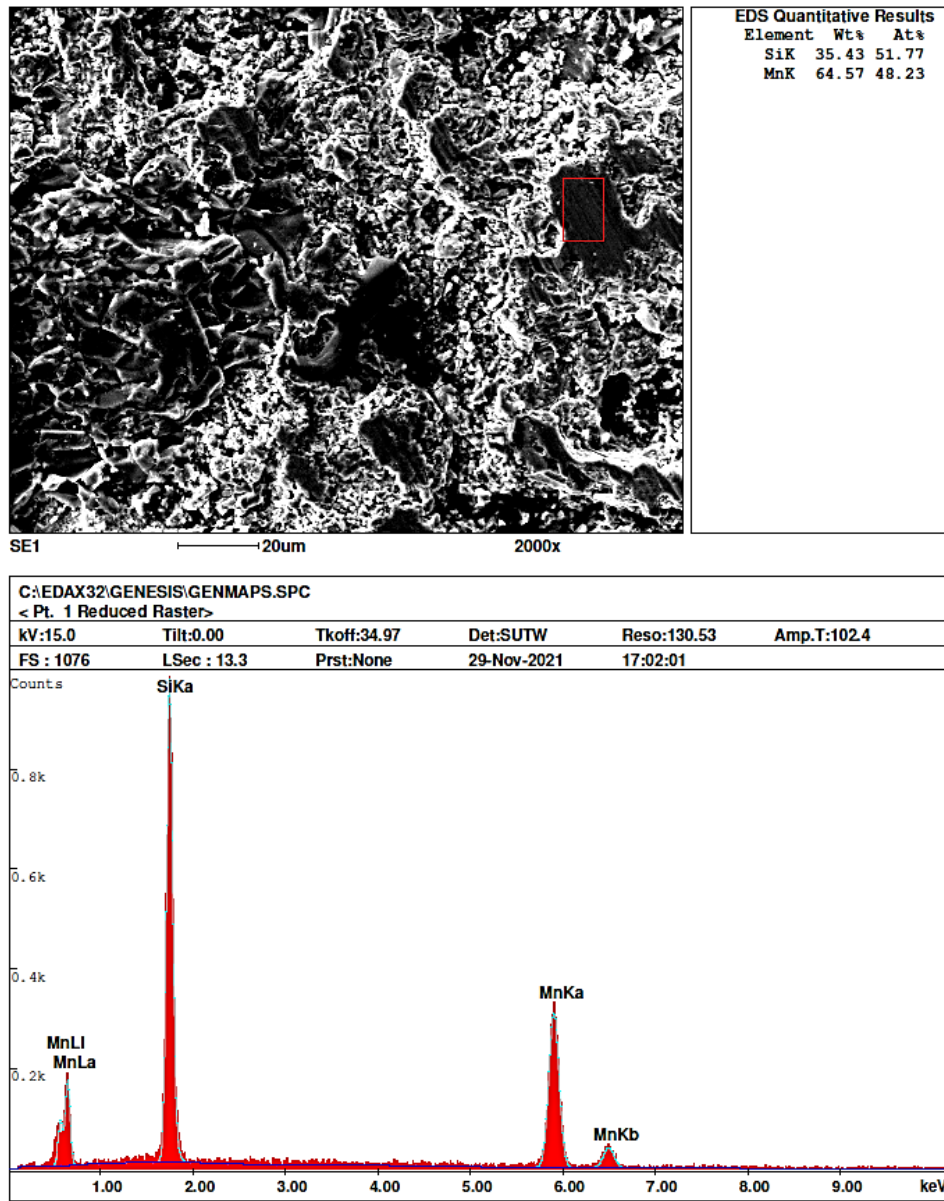


Fig. 4. Image of the Mn₄Si₇ target obtained with a scanning electron microscope

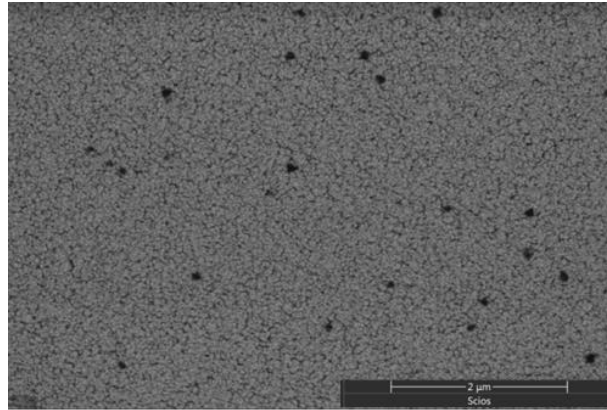
The results obtained show that the targets were formed from Mn₄Si₇ and CoSi silicides. It is the selection of these silicides that has good thermal efficiency and is rarely used in production. Of course, a small percentage of foreign impurities is present in the surface and near-surface layers, and the amount of oxygen on the surface is quite large. As far as we know, high vacuum conditions are not used in the formation of the target, and the appearance of foreign atoms on the surface as a result of exposure to subsequent open air is natural. We can only reduce their percentage, but we cannot completely clean them up.

In conclusion, the optimal regimes for the formation of *p* - type Mn₄Si₇ and *n* - type CoSi targets were determined, which were used to create device structures.

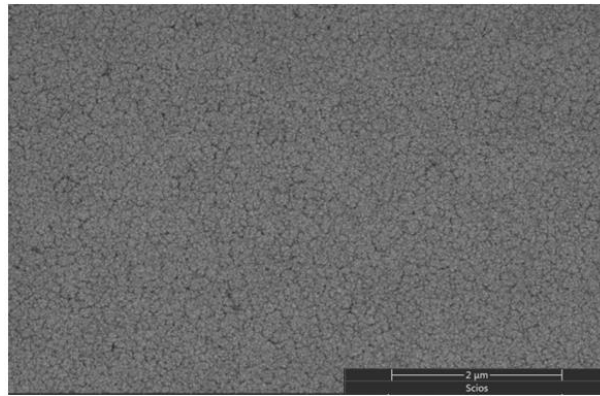
The band width of the $\text{Mn}_4\text{Si}_7/\text{SiO}_2$ film was measured on a high-precision HR-4000 spectrometer according to the law of light reflection. It is known that the thermoelectric figure of merit of a material is a dimensionless quantity and is determined by formula (1) (Pitarch *et al.*, 2018; Stevens *et al.*, 2010; Yin & Tiwari, 2021).

$$ZT = \frac{S^2\sigma T}{k} = \frac{S^2\sigma T}{k_l + k_e} \quad (1)$$

The Mn_4Si_7 film formed by magnetron sputtering is in the amorphous state before thermal heating, which we can identify from (Fig. 5a).



a)



b)

Fig. 5. Mn_4Si_7 film before heating a) and after heating at a pressure of $P = 10^{-3}$ Pa at a temperature of $T = 800$ K b)

Silicon and manganese atoms deposited on silicon oxide almost completely cover the substrate. As a result of experiments with an amorphous film, we see that the film has metallic properties. In the amorphous state, the resistance of the film is greater than the resistance in the polycrystalline state. This is due to the fact that the bond between the manganese and silicon atoms is very weak and there are point defects on the surface areas that are not completely covered. After the film is annealed, point defects on the surface disappear, the manganese and silicon atoms form a bond, and the resulting structure has semiconductor properties. The formation of the Mn_4Si_7 film was carried out by magnetron

sputtering (sputtering lasted 15 minutes). During this time, an amorphous Mn_4Si_7 film 250 nm thick was formed. But during the next heat treatment, i.e., after heating at a temperature of 800 K, there is a change in the thickness and concentration of the resulting polycrystalline Mn_4Si_7 film.

On fig. 6 shows the morphology and composition of the formed $\text{CoSi}/\text{SiO}_2/\text{Si}$ thin silicon film obtained using a scanning electron microscope (Solomkin *et al.*, 2019). The surface shown in fig. 6 shows the morphology of a CoSi silicon film with smooth but known defects. The main reason for the formation of these defects is that, when CoSi is sputtered, various nanosized pieces of CoSi are deposited on the substrate. To minimize these defects and the amount of unbound Co and Si atoms, the film is heated at 700 K for 1 hour in high vacuum (10^{-6} Pa).

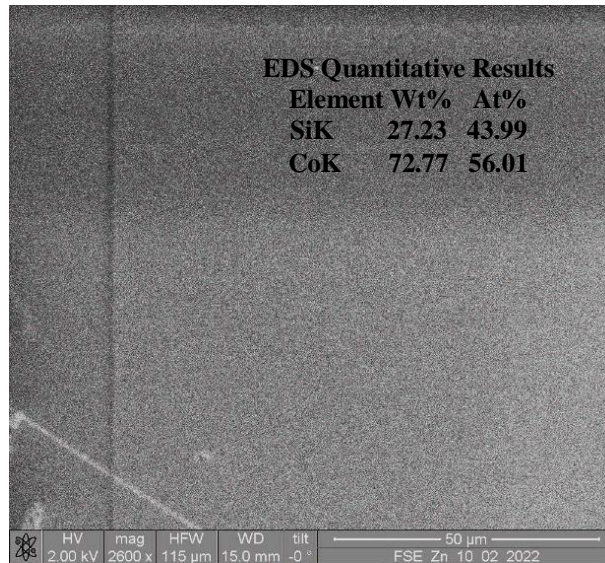


Fig. 6. Surface morphology and composition of the CoSi film on the SiO_2 surface, obtained by SEM

To create effective receivers of thermal radiation (thermoelectric converters) of various designs, it is necessary to form a series connection of a p-type manganese silicide layer and an n-type cobalt (or metal) silicide conductivity layer, to the final and initial parts of which conductors can be soldered. Since it is desirable to make the dimensions of thermal radiation receivers as small as possible, but reproducible and convenient in production, the size of the main part of the transducers was chosen within 5–6 mm. For ease of manufacture and the ability to quickly change the topology of photomasks, the option of flexible film templates (special phototechnical film) was chosen. Today, this option is widely used in production.

The most suitable materials for the manufacture of photomasks (depending on the task) turned out to be phototechnical reproduction films of the FT type with different indicators. Convenient and modern material AGFA Recording HNS photographic film based on polyester for exposure with a red laser or a red laser diode at a wavelength of 630 - 670 nm. The film is processed on automatic processing machines with high productivity.

The proposed topological scheme of film photomasks should take into account the following:

- the accuracy of manufacturing elements on the film cannot be better than 10 - 20 microns;
- the roughness of the edge of the image can reach 5 - 10 microns;
- during production (drawing), the film can be stretched, including diagonally, topological patterns should be located closer to each other in one zone of the rolled film;
- it is necessary to provide for the combination of topological layers (for the design of special alignment marks).

Thus, the first tests showed that if the topology of sections of manganese silicide is first formed, and a metal layer is applied on top, then a continuous upper layer of metal does not allow you to see the lower topological pattern and it is impossible to combine the layers (patterns). To do this, it is necessary to move the alignment marks outside the area of the working areas and take measures to ensure that the primary alignment mark is not covered with a layer of metal.

The next step is to prepare a metal mask for structures. Thin steel sheets were used to make the masks, and the required dimensions were created using a laser. The diameter of the resulting device in the form of a camomile is 12.5 mm (Fig. 7 *a* and *b*).

The next step is the formation of the device structure in the magnetron sputtering device. This requires a suitable substrate (mica, glass-ceramic or $\text{SiO}_2/\text{Si}(111)$), which must be a dielectric substrate.

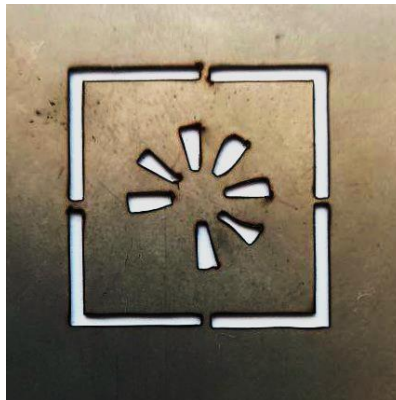
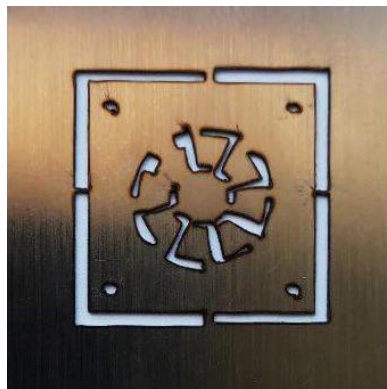
*a)**b)*

Fig. 7. (*a*) to obtain p-type Mn_4Si_7 and (*b*) to form an n-type CoSi structure

Photomasks were prepared to create instrument structures from different materials. The fabricated photomasks (2 types) were used to create instrumental structures. Each photomask type will also have two different representations. In particular, the photomask shown in Fig. 7 shows separate *p*- and *n*- type molds that were used in the magnetron sputtering apparatus.

Photolithography is a technological process based on the use of photochemical phenomena occurring in a photoresist layer deposited on a substrate during treatment with ultraviolet radiation through a mask (photomask), and then ideas about the formation of a mask in a layer through a photoresist mask and wrapping the substrate.

The spin technology is mainly used, in which a thin layer of photoresist is applied to the substrate on one side. The advantage of this method is the possibility of applying a layer of photoresist to small areas of the surface with a high degree of uniformity in thickness. The dependence of the thickness of the photoresist layer h remaining on the surface on the centrifuge speed ω and the kinematic viscosity of the photoresist η on the generally accepted speed range is determined by the dependence of the form: $h = K \cdot \sqrt{\eta/\omega}$, where the substances are in solution. To apply photoresists to plates of any shape, you can use a variable table with a rotation time of 5 to 60 s and very simple centrifuges with speed control in the range of 300 - 3000 rpm. (Igamov *et al.*, 2021).

At present, contact photolithography is widely used and is the most advanced method, characterized by high productivity and low cost. Relatively high resolutions are achieved due to the close contact of the photomask with the substrate. Elements with a size of 1.0 - 1.5 μm can be transferred onto a photolayer of a positive photoresist with a thickness of 0.5 - 0.7 μm .

To process any type of photoresist, mercury lamps or laser processing must be used. There are also UV lamps based on UV LEDs, such as the NDS 312/308, which provide high power at a wavelength of approximately 365 nm.

The correct exposure depends on the type of photomask, the thickness of the photoresist and the process parameters. The main condition for a high-quality exposure operation is to determine the optimal exposure that provides the best quality and reproducibility of the results of the photolithographic process. In practice, a number of control processes are carried out to determine the optimal exposure, exposures are made at different shutter speeds, they are developed in a standard way, and the resulting image is controlled using microscopes MII-4, MIM-7, etc.

3. Results and discussion

The mask is placed on the substrate and for 15 minutes under a pressure of 10^{-4} Pa (after the introduction of Ar^+ ions), the highest manganese silicide is sprayed using the magnetron sputtering method. This allows you to get the *p*-type structure of the instrument structure. After turning off the magnetron sputtering device, the formed structure is carefully examined; the main reason for such an inspection can be explained by the formation of a clear border on the sides of the formed structure (Fig. 8). The process of development of photoresists consists in the complete removal of unnecessary areas of the photoresist from the surface of the substrate after exposure. As a result, only a protective relief of the desired configuration remains on the surface (the surface for etching is

exposed). The development of layers of positive photoresist is usually carried out in slightly alkaline solutions, which leads to the removal of exposed areas. During development, a chemical reaction occurs and the indencarboxylic acid obtained as a result of exposure turns into a highly soluble salt, which is then easily washed out. After spraying, the surface of the photoresist changes from a hydrophobic state to a hydrophilic one, so the dusty areas are well wetted by the manufacturer. As developers, water-alkaline solutions are used (0.3-0.5% alkaline potassium solution, 1-2% trisodium phosphate solution).

The placement of the second mask requires more precision than the placement of the first mask, because in the first magnetron the sputtered layer must form contacts in the right part of the higher silicide-manganese film. The structure placed in the magnetron sputtering device was re-sputtered with cobalt silicide, and the structure was finally formed (Fig. 9).

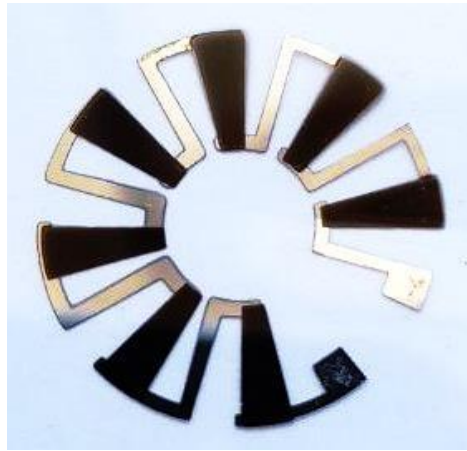


Fig. 8. Sputtered Mn_4Si_7 side of the device in the form of a camomile



Fig. 9. Sputtered $CoSi$ side of the device in the form of a camomile

The next process is the heat treatment of the manufactured device. To do this, p - type Mn_4Si_7 and n - type $CoSi$ structures formed by magnetron sputtering are heated to a temperature of $600\text{ }^\circ\text{C}$ at a pressure of 10^{-6} Pa (Fei *et al.*, 2021; Klechkovskaya *et al.*, 2021).

The task of the final stage of photolithography is the formation of a topological coating on the material being processed. For this, chemical etching processes are mainly used (dissolution of a material based on the interaction of this material with an etching solution). Using the method of magnetron sputtering, structures were created that can be used in thermal radiation receivers. The mechanism of structure formation has been developed.

4. Conclusions

This paper shows that various types of structures were created by magnetron sputtering of a Mn_4Si_7 *p*-type and CoSi *n*-type target using a photomask and that these structures can be used in thermal radiation detectors. The optimal modes of formation of Mn_4Si_7 *p*-type and CoSi *n*-type targets are determined. Mn_4Si_7 and CoSi targets for the magnetron sputtering device have been created. Photomasks have been prepared to create an instrument structure from different materials. Photomasks (2 types) were made, which were used to create instrumental structures. A structure was created using the magnetron sputtering method, which could be used in thermal radiation receivers. The mechanism of structure formation has been developed.

References

- Asanabe, S., Shinoda, D., Sasaki, Y. (1964). Semimetallic properties of $\text{Co}_{1-x}\text{Fe}_x\text{Si}$ solid solutions. *Physical Review*, 134, A774.
- Agayev, T., Imanova, G., & Aliyev, A. (2022). Influence of gamma radiation on current density and volt-ampere characteristics of metallic zirconium. *International Journal of Modern Physics B*, 36(19), 2250115.
- Bekpulatov, I.R., Imanova, G.T., Kamilov, T.S., Igamov, B.D., & Turapov, I.Kh. (2022). Formation of n-type *cosi* monosilicide film which can be used in instrumentation. *International Journal of Modern Physics B*, <https://doi.org/10.1142/S0217979223501643>.
- Dubov, V.L. (2019). Formation, structure, optical and photoelectric properties of textured BaSi_2 films on Si(111) and heterostructures based on them, Dissertation. Blagoveshchensk, 124, 67-70.
- Donaev, S.B., Tashatov, A.K., & Umirzakov, B.E. (2015a). Effect of Ar^+ -ion bombardment on the composition and structure of the surface of $\text{CoSi}_2/\text{Si}(111)$ nanofilms. *Journal of Surface Investigation: X-ray, Synchrotron and Neutron Techniques*, 9(2), 406-409.
- Donaev, S.B., Umirzakov, B.E., Tashmukhamedova, D.A. (2015b). Electronic structure of $\text{Ga}_{1-x}\text{Al}_x\text{As}$ nanostructures grown on the GaAs surface by ion implantation. *Technical Physics*, 60(10), 1563-1566.
- Fedorov, M.I., Zaitsev, V.K. (1991). In: *CRC Handbook of Thermoelectrics*, ed. by D.M. Rowe (CRC Press, N.Y.), 321 p.
- Fei, J., Wang, H., & Fang, Y. (2021). Novel Neural Network Fractional-Order Sliding-Mode Control With Application to Active Power Filter. *IEEE Transactions on Systems, Man, and Cybernetics: Systems*, 99, 1-11.
- Hashimoto, K., Kurosaki, K., Imamura, Y., Muta, H., & Yamanaka, S. (2007). Thermoelectric properties of BaSi_2 , SrSi_2 , and LaSi . *Journal of Applied Physics*, 102, 063703.
- Hashimoto, K., Kurosaki, K., Muta, H., & Yamanaka, S. (2008). Thermoelectric Properties of La-Doped BaSi_2 . *Materials Transactions*, 49(8), 1737-1740.
- Igamov, B.D., Kamardin, A.I., Kamilov, T.S., Bekpulatov, I.R., Turapov, I.Kh., & Igamova, D.D.

- (2021). Evaluation of the thickness of vacuum metal and semiconductor coatings using computer programs. *Technical Science and Innovation*, 4(10), 255-263.
- Imai, M., Kikegawa, T. (2003). Phase transitions of alkaline-earth-metal disilicides $M_{AE}Si_2$ ($M_{AE} = Ca, Sr, \text{ and } Ba$) at high pressures and high temperatures. *Chemistry of Materials*, 15, 2543-2551.
- Imanova, G., Bekpulatov, I. (2021a). Investigation on the electronic structure of nanosized barium monosilicide films produced by low-energy implantation of Ba^+ ions in Si. *American Journal of Nano Research and Applications*, 9(4), 32-35.
- Imanova, G.T., Agayev, T.N., 7 Jabarov, S.H. (2021b). Investigation of structural and optical properties of zirconia dioxide nanoparticles by radiation and thermal methods. *Modern Physics Letters B*, 35(02), 2150050.
- Isakhanov, Z.A., Umirzakov, B.E., Ruzibaeva, M.K., & Donaev, S.B. (2015). Effect of the O_2^+ -ion bombardment on the TiN composition and structure. *Technical Physics*, 60(2), 313-315.
- Kamilov, T.S., Rysbaev, A.S., Klechkovskaya, V.V., Orekhov, A.S., Igamov, B.D., & Bekpulatov, I.R. (2019). The influence of structural defects in silicon on the formation of photosensitive $Mn_4Si_7-Si(Mn)-Mn_4Si_7$ and $Mn_4Si_7-Si(Mn)-M$ heterostructures. *Applied Solar Energy*, 55(6), 380-384.
- Kishino, S., Imai, T., Iida, T., Nakaishi, Y., Shinada, M., Takanashi, Y., & Hamada, N. (2007). Electronic and optical properties of bulk crystals of semiconducting orthorhombic $BaSi_2$ prepared by the vertical Bridgman method. *Journal of Alloys and Compounds*, 428, 22-27.
- Klechkovskaya, V.V., Rysbaev, A.S., Kamilov, T.S., Bekpulatov, I.R., Igamov, B.D., & Turapov, I.Kh. (2021). Formation of Mn_4Si_7 thin films on various substrates by magnetron sputtering and pulsed laser deposition. *Uzbek Journal of Physics*, 22(3), 43-48.
- Mavrokefalos, A., Pettes, M.T., Zhou, F., Shi, L. (2007). Four-probe measurements of the in-plane thermoelectric properties of nanofilms. *The Review of Scientific Instruments*, 78(3), 034901.
- Morita, K., Inomata, Y., & Suemasu, T. (2006). Optical and electrical properties of semiconducting $BaSi_2$ thin films on Si substrates grown by molecular beam epitaxy. *Thin Solid Films*, 508, 363-366.
- Normurodov, M.T., Rysbaev, A.S., Bekpulatov, I.R., Normurodov, D.A., & Tursunmetova, Z.A. (2021). Formation and electronic structure of barium-monosilicide- and barium-disilicide films. *Journal of Surface Investigation: X-ray, Synchrotron and Neutron Techniques*, 15, 211-215.
- Pitarch, B.B., Gonjal, J.P., Powell, A., Ziolkowski, P., & Canadas, J.G. (2018). Thermal conductivity, electrical resistivity, and dimensionless figure of merit (ZT) determination of thermoelectric materials by impedance spectroscopy up to 250 °C. *Journal of Applied Physics*, 124(2), 025105.
- Pshenay-Severin, D.A., Ivanov, Y.V., Burkov, A.A., & Burkov, A.T. (2018). Band structure and unconventional electronic topology of CoSi. *Journal of Physics: Condensed Matter*, 30, 135501.
- Rysbaev, A.S., Khujaniyozov, J.B., Bekpulatov, I.R., Rakhimov, A.M. (2017a). Method for additional purification of the surface of Si(111) single crystal. *Journal of Surface Investigation: X-ray, Synchrotron and Neutron Techniques*, 11(5), 994-999
- Rysbaev, A.S., Khujaniyozov, J.B., Bekpulatov, I.R., Rakhimov, A.M., Pardaev, O.R. (2017b). Effect of thermal and laser annealing on the atom distribution profiles in Si(111) implanted with P^+ and B^+ ions. *Journal of Surface Investigation: X-ray, Synchrotron and Neutron Techniques*, 11(2), 474-479.
- Shakouri, A. (2011). Recent developments in semiconductor thermoelectric physics and materials. *Annual Review of Materials Research*, 41(1), 399-431.
- Solomkin, F.Yu., Orekhov, A.S., Novikov, S.V., Arkharova, N.A., Isachenko, G.N., Zaitseva, N.V., Sharenkova, N.V., Samunin, A.Yu., Klechkovskaya, V.V., & Burkov, A.T. (2019).

- Structure and thermoelectric properties of CoSi obtained from a supersaturated solution-melt in Sn. *Physics and Technology of Semiconductors*, 53(6), 32-35.
- Stevens, K.R., Kanatzidis, M.G., Johnsen, S., & Girard, S.N. (2010). Investigation of the thermoelectric properties of metal chalcogenides with SnSe. *Nanoscope*, 7, 52-57.
- Tahir, A.B., Aqsa, I.A., Bilal, T.M., Ijaz, T.M. (2020). Interfaces and surfaces. *Chemistry of Nanomaterials. Fundamentals and Applications*, 51-87.
- Tursunmetova, Z.A., Imanova, G., Bekpulatov, I. (2022). Method for low-temperature vacuum-thermal cleaning of surface single crystals Si and GaAs. *Journal of Polytechnic*, 25(2), 921-927.
- Umirzakov, B.E., Bekpulatov, I.R., Turapov, I.Kh., & Igamov, B.D. (2022). Effect of deposition of submonolayer Cs coatings on the density of electronic states and energy band. *Journal of Nano- and Electronic Physics*, 14(2), 02026.
- Umirzakov, B.E., Donaev, S.B. (2017). On the creation of ordered nuclei by ion bombardment for obtaining nanoscale Si structures on the surface of CaF₂ films. *Journal of Surface Investigation: X-ray, Synchrotron and Neutron Techniques*, 11(4), 746-748.
- Vaqueiro P., Powell, A.V. (2010). Recent developments in nanostructured materials for highperformance thermoelectrics. *Journal of Materials Chemistry*, 20(43), 9577.
- Yin, Y., Tiwari, A. (2021). Understanding the effect of thickness on the thermoelectric properties of Ca₃Co₄O₉ thin films. *Scientific Reports*, 11(11), 6324.
- Yoneyama, T., Okada, A., Suzuno, M., Shibutami, T., Matsumaru, K., Saito, N., Yoshizawa, N., Toko, K., Suemasu, T. (2013). Formation of polycrystalline BaSi₂ films by radio-frequency magnetron sputtering for thin-film solar cell applications. *Thin Solid Films*, 534, 116-119.